5th International Symposium on Three-Dimensional Electromagnetics
Sapporo, Japan, May 7–9, 2013

# A novel 3-D MT inverse solver: its implementation and outlook

Jenneke Bakker and Alexey Kuvshinov
Institute of Geophysics, ETH Zurich, Switzerland

## SUMMARY

We are developing a modular three-dimensional (3-D) magnetotelluric (MT) inverse solver. As a forward modeling engine an integral equation (IE) approach is used and the inversion itself is based on an iterative gradient-type optimization method. The adjoint approach is invoked to calculate the gradient of the misfit. Besides the impedance tensor, also the horizontal magnetic tensor, tippers and the phase tensor can be employed. Here, we present the implementation and an outlook for extensions of our inverse solver.

**Keywords:** magnetotellurics, 3-D inversion, adjoint approach

## INTRODUCTION

The first three-dimensional (3-D) magnetotelluric (MT) inverse solver was developed by Mackie and Madden (1993). About a decade later, several other 3-D MT inverse solvers were developed (Newman and Alumbaugh (2000), Haber, Ascher, and Oldenburg (2004), Siripunvaraporn, Egbert, Lenbury, and Uyeshima (2005), Sasaki and Meju (2006), Avdeev and Avdeeva (2009), Zhdanov, Green, Gribenko, and Cuma (2010), Egbert and Kelbert (2012), Zhang, Koyama, Utada, Yu, and Wang (2012)). The main differences between these solvers lie in the forward engine used to calculate the electromagnetic (EM) fields, the optimization method used for the inversion and the response functions inverted.

As the inverse solvers of Avdeev and Avdeeva (2009) and Zhang et al. (2012), our inverse solver is also based on an integral equation (IE) forward engine, uses a quasi-Newton optimization method to minimize the objective function, and the gradient of the misfit is calculated via the adjoint approach. However, in our inverse solver, the IE approach of the forward model engine is exploited by isolating the calculation of the Green's tensors and thereby accelerating the inversion. Another difference is the more flexible parametrization of the inverse problem such that can be accounted for an irregular distribution of the site locations. Furthermore, our solver is built in a modular way enabling an easy exchange of the response function inverted or implementation of an alternative optimization method.

## FORWARD ENGINE AND ITS MODIFICATIONS

As a starting point for the development of our inverse solver, the forward engine *x3D* (Avdeev, Kuvshinov, Pankratov, and Newman (1997, 2002)) was substantially modified. Modifications include conversion of *x3D* from FORTRAN77 to FORTRAN90 enabling an easier integration within a modular inverse solver. In addition, dynamic memory allocation is used instead of static memory allocation.

IE based forward engines use the fact that any 3-D conductivity distribution can be represented by 3-D conductivity scatterers $\sigma(x, y, z)$ embedded in a 1-D conductivity section $\sigma(z)$. For this 1-D background section, explicit expressions of the Green's tensors can be obtained ( e.g. Avdeev et al. (1997)). These Green's tensors are independent of the 3-D conductivity distribution, which is the subject of interest in the inversion process. This is exploited in our inverse solver by calculating the Green's tensors only once. Throughout the inversion, the 1-D background section is fixed and the Green's tensors are not re-calculated.

In *x3D* the dipole excitation is realized via an integral over the cell containing the source. For controlled source experiments, where the field of interest is far away from the source, this works without problems. However, if the field of interest is located close to the source, as could be the case for the gradient calculations, the EM fields could contain numerical noise. Therefore, the option for actual electric and magnetic dipole excitations is added to the forward engine.

## RESPONSE FUNCTIONS USED FOR THE INVERSION

Besides the commonly used impedance tensor, also the phase tensor, the horizontal magnetic tenor and the tippers are employed in our inverse solver. Additionally, joint inversion of two or more types of response functions is possible. Explicit expressions for the gradient calculations of the misfit for the different response functions, can be found in Pankratov and Kuvshinov (2010).

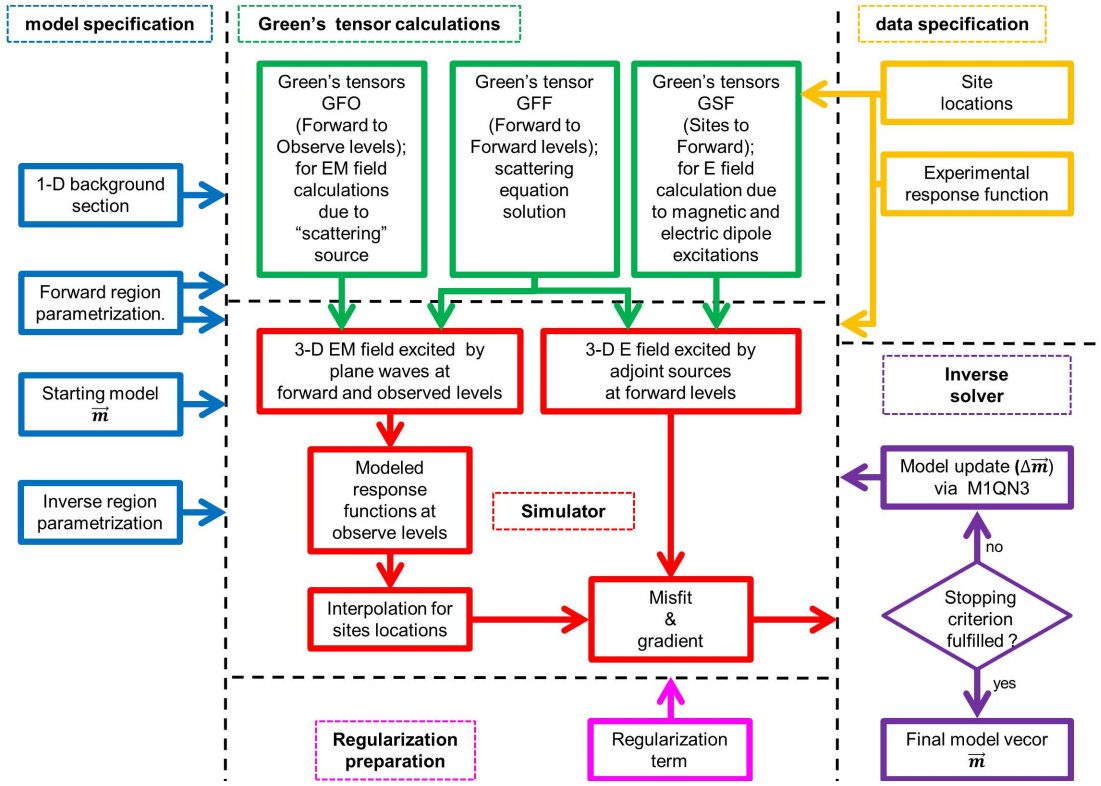


**Figure 1.** Flowchart of the inversion algorithm. The algorithm consists of six blocks: 1. model specification; 2. data space specification; 3. Green's tensor calculations; 4. simulator; 5. inverse solver; 6. regularization preparation. The main block of the inverse code is the simulator, which receives input from the five other blocks.

## INVERSE SOLVER

A schematic representation of our 3-D inversion solver is shown in Figure 1. The inverse code consists of six blocks. Within the model specification block (indicated in blue), the parametrization of the forward, observe and inverse domains are defined. The inverse domain allows for a flexible parametrization depending on the spatial distribution of the site locations. The starting model is defined as well within the model specification block.

The second block is the data specification block (indicated in yellow), containing the experimental responses and information about the site locations.

Information from both the data and the model specification blocks is needed for the calculation of the Green's tensors (indicated in green). There are three different Green's tensors to be calculated. First of all, the Green's tensor to solve the scattering equation within the forward modeling domain (GFF). Secondly, the Green's tensors to calculate the EM field at observe levels (GFO). Lastly, the Green's tensors to compute the 1-D background electric field in the forward modeling domain excited by both the electric and the magnetic adjoint dipole source located at the sites (GSF).

Within the simulator (indicated in red), the misfit and its gradient are calculated via the adjoint approach. Two different modules are introduced for these calculations. One module solves Maxwell's equations for a plane wave excitation and calculates the electric field in the forward modeling domain and the total EM field at observe levels. The second module solves the same equations for the adjoint electric and magnetic dipole excitations providing the electric field in the forward modeling domain. These two modules of the simulator are parallelized over both frequency and polarization. An additional module is introduced to calculate the response functions at observe levels and interpolate these response functions to the site locations.

The regularization preparation block (indicated in magenta) provides a constraint on the model parameters. This block consists of information about the smoothing term, its gradient and determines the value of the regularization parameter $\lambda$.

The outputs of the simulator, the misfit plus regularization term and their gradients, are inputs for the inverse solver (indicated in purple). If the stopping criterion is not fulfilled, a model update is found via the routine M1QN3 developed by Gilbert and Lemarechal (1989) using the limited memory quasi-Newton (LMQN) (Nocedal & Wright,

2006). The new model vector in turn is input for the simulator and the misfit and its gradient are re-calculated. To ensure that the conductivity remains positive throughout the inversion, the model parameter inverted for is $\log\sigma$ instead of $\sigma$. It is possible that during an iteration, the optimization routine needs information on the problem and an additional communication is taking place between the simulator and M1QN3. The iterative process is repeated until the stopping criterion is fulfilled.

## OUTLOOK

In MT experiments, one inverts for real valued conductivities. However, when displacement currents or induced polarization effects are considered, one is interested in complex valued conductivities. Extension of our inverse solver for complex valued conductivities is rather straightforward.

Most MT inverse solvers work with scalar valued conductivities. However, there are situations where an anisotropic conductivity distribution should be considered. We plan to include conductivity distributions which are represented by a second order tensor.

MT data can be recorded in environments with a well pronounced topography or bathymetry. Our inverse solver can easily deal with these scenarios.

Implementation of controlled source experiments within the inverse solver is planned as well.

Ultimately, we would like to know how good the model parameters are resolved. The Hessian matrix contains information about the model resolution and can be computed via an adjoint sources approach (Pankratov & Kuvshinov, 2013). Implementation of these adjoint calculations of the Hessian matrix and using the result to quantify the model resolution, is also planned.

## ACKNOWLEDGEMENTS

This work has been supported by ETH grant No. ETH-3010-3.

## REFERENCES

Avdeev, D., & Avdeeva, A. (2009). 3D magnetotelluric inversion using a limited-memory quasi-Newton optimization. *Geophysics*, *74*(3), F45-F57.

Avdeev, D., Kuvshinov, A., Pankratov, O., & Newman, G. (1997). High-performance three-dimensional electromagnetic modelling using modified Neumann series. Wide-band numerical solution and examples. *Journal of Geomagnetism and Geoelectricity*, *49*(11-12), 1519-1539.

Avdeev, D., Kuvshinov, A., Pankratov, O., & Newman, G. (2002). Three-dimensional induction logging problems, Part I: An integral equation solution and model comparisons. *Geophysics*, *67*(2), 413-426.

Egbert, G. D., & Kelbert, A. (2012). Computational recipes for electromagnetic inverse problems. *Geophysical Journal International*, *189*(1), 251-267.

Gilbert, J., & Lemarechal, C. (1989). Some numerical experiments with variable-storage quasi-Newton algorithms. *Mathematical programming*, *45*(3), 407-435.

Haber, E., Ascher, U., & Oldenburg, D. (2004). Inversion of 3D electromagnetic data in frequency and time domain using an inexact all-at-once approach. *Geophysics*, *69*(5), 1216-1228.

Hautot, S., Tarits, P., Whaler, K., Le Gall, B., Tiercelin, J., & Le Turdu, C. (2000). Deep structure of the Baringo Rift Basin (central Kenya) from three-dimensional magnetotelluric imaging: Implications for rift evolution. *Journal of Geophysical Research*, *105*(B10), 23493-23518.

Mackie, R., & Madden, T. (1993). Three-Dimensional magnetotelluric inversion using conjugate gradients. *Geophysical Journal International*, *115*(1), 215-229.

Newman, G., & Alumbaugh, D. (2000). Three-dimensional magnetotelluric inversion using non-linear conjugate gradients. *Geophysical Journal International*, *140*(2), 410-424.

Nocedal, J., & Wright, S. (2006). *Numerical optimization*. Springer.

Pankratov, O., & Kuvshinov, A. (2010). Fast calculation of the sensitivity matrix for responses to the Earth's conductivity: General strategy and examples. *Izvestiya-Physics of the solid Earth*, *46*(11), 1017-1018.

Pankratov, O., & Kuvshinov, A. (2013). General formalism for the efficient calculation of the hessian matrix of em data misfit based upon adjoint approach. *Geophysical Journal International,*(submitted).

Sasaki, Y., & Meju, M. (2006). Three-dimensional joint inversion for magnetotelluric resistivity and static shift distributions in complex media. *Journal of Geophysical Research*, *111*(B5).

Siripunvaraporn, W., Egbert, G., Lenbury, Y., & Uyeshima, M. (2005). Three-dimensional magnetotelluric inversion: data-space method. *Physics of the Earth and Planetary Interiors*, *150*(1-3), 3-14.

Zhang, L., Koyama, T., Utada, H., Yu, P., & Wang, J. (2012). A regularized three-dimensional magnetotel-

luric inversion with a minimum gradient support constraint. *Geophysical Journal International*, *189*(1), 296-316.

Zhdanov, M. S., Green, A., Gribenko, A., & Cuma, M. (2010). Large-scale three-dimensional inversion of EarthScope MT data using the integral equation method. *Izvestiya, Physics of the solid Earth*, *46*(8), 670-678.